

## Performance of a Solar Chimney with a Dual-Cavity System

H. Jones, P. Elgindy, C. Lei and K. Chauhan

School of Civil Engineering  
University of Sydney, New South Wales 2006, Australia

### Abstract

An experimental investigation of thermal flows in a dual-cavity solar chimney is presented here. The cavity separator is a radiative surface which absorbs incident radiation thereby inducing thermal boundary layers on both sides of the surface. A theatre lamp is used to simulate the typical level of insolation in an Australian summer climate. Thermistors are used to measure the temperature along the height of the radiative foil. Five tinting arrangements were tested to investigate whether this would induce a vertical temperature differential that would be beneficial to the air flow. Arrangements with half of the glass pane with tinting that transmits just 2.25% of visible light provided similar results to a clear glass pane. Therefore, a gradual decrease in tint was not conducive to increasing airflow. Between the single and dual cavity tests, the single cavity exhibited a 29% increase in velocity. However, considering that the cross-sectional area was halved, this indicates that the dual cavity has the potential to increase flow through further refinement.

### Introduction

Australians are spending, on average, greater than 90% of time indoors, therefore good ventilation is essential for health, safety and thermal comfort [7]. With 49% of households using reverse cycle air conditioning [6], natural ventilation provides an attractive alternative. However, to be considered viable it should provide consistent air exchange rates comparable to a forced ventilation methods. Natural ventilation is dependent upon external factors to produce the pressure differential required to drive the flow. The solar chimney provides a hot air solar collector to cause the occurrence of natural convection due to the increasing buoyancy of the air within the chimney. This then drives air flow.

The basic operation and design of a solar chimney that is reliant on solar-induced buoyancy-driven convection constrained within a vertical channel is well established. This research seeks to derive a relationship between the temperature differential through the chimney and the airflow rate. This research also seeks to improve the solar chimney's flow rate performance by taking a new approach to the solar chimney's design – the internal radiative wall and the glass outer wall. This study tests the effect of mounting a radiative surface in the centre of the cavity and parallel to the glass outer wall, in order to create a boundary layer on either side of the radiative wall and potentially double the amount of air entrained by the convective flow as illustrated in Figure 1. Mounting the radiative surface in the centre of the cavity is also intended to reduce the amount of heat that would be transferred into the building by conduction if the wall of the building itself were used as the radiative surface (which could counteract the cooling purpose of the solar chimney). Furthermore, this study will test the effect of graduated tinting on the glass wall to create a pressure driven flow through the chimney that works in tandem with the natural convection flow to increase the ventilation rate.

Previous research has also sought a mathematical relationship between measurable quantities and air flow performance, either based on a room with certain openings and air temperature [5,8] or as a thermal network of heat transfers inside the solar chimney itself [22]. The geometry of the chimney has been a frequent topic of concern, particularly regarding the size of the air gap between the glass and the radiative surface [10,11,12,14] and the possibility of back flow; the height-to-width ratio of 10 recommended by Bouchair et al. [10,11] has been adopted for this study. This study's comparison between the experimental method of assessing geometric variables and a numerical model of heat transfers has much precedent [4,9,23], but the application of this to the role of boundary layers in the specific context of solar chimneys has been rare. Khanal & Lei [20] focused on scaling of the boundary layer in a solar chimney but most other relevant boundary layer work simply considers flat plates, whether it is another scaling analysis [24] or numerical simulations of aiding and opposing freestreams [2,3] and forced convection [25]. The theory of the boundary layer's growth due to entrainment has been examined [13,17] but the possibility of its application to augmenting the flow rate in a solar chimney appears to have been hitherto neglected in the literature.

The motivation for the present study is to improve ventilation efficiency, a topic that has been tested in terms of air change per hour achieved by solar chimneys [4,9] and also in general terms of thermal comfort and qualitative human experience [1,15,16,18,19,21]. The evaluation of thermal comfort in the room or building being ventilated is beyond the scope of the present research. Assessment of the performance of this solar chimney in terms of thermal comfort effectiveness will be one of the aims of future work on this study. While many aspects of the design and performance of solar chimneys have been studied in great detail, there is a gap in the existing literature regarding both the dual-cavity solar chimney and the use of graduated tinting to produce a vertical differential in foil temperature to induce upwards pressure driven flow in addition to buoyancy driven flow induced by natural convection.

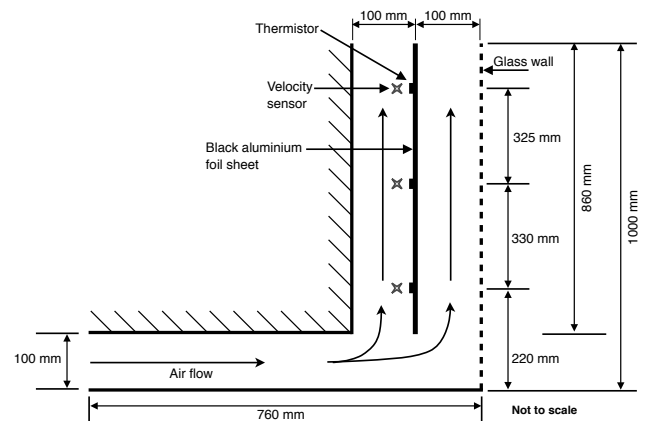


Figure 1. Schematic of the experimental set-up (not to scale).

## Experimental Apparatus

The experimental apparatus is 1000 mm high with cavity dimensions of 300 mm × 100 mm (width × depth) each, and the radiative surface is 860 mm high, shown in Figure 1. Experiments can be conducted under controlled indoor conditions or situated outside in an optimal position for receiving sunlight to test the solar chimney's operation under real-world conditions. The surface that absorbs and reradiates the incident solar radiation is made of black aluminium foil held taut between two frame struts. The cavities can be blocked at the base of the chimney cavity both vertically and horizontally, to allow for a variety of cavity arrangements. Using a Selecon Rama 6" Fresnel theatre lamp as a substitute heat source to simulate solar radiation, testing was undertaken in the Fluids Laboratory at The University of Sydney. As indicated in Figure 2, tests were performed on several arrangements of tinted film on the glass panel, and opening or blocking the rear cavity to test the dual and single cavity layouts. Surface thermistors (SA1-TH-44006 from Omega Labs) were mounted on the radiative surface to measure its longitudinal temperature variation over the course of the experiment. The thermistors were mounted at heights of 220mm, 550mm and 875mm above the cavity's base. Sensors to measure both air velocity and ambient temperature (Wind Sensor Revision P thermal anemometers from Modern Device) were mounted in the rear cavity at the same heights as the thermistors and 40 mm from the radiative surface, to measure the speed of the airflow through the chimney. All sensors were placed behind the radiative surface to eliminate the effects of direct insolation on the sensors (except in configuration F, when the air velocity in the front cavity was the target of measurement and the anemometers were therefore moved to that cavity). The data from these sensors was gathered at 100 Hz by a National Instruments data acquisition system comprising 24-bit NI-9239 modules mounted in a cDAQ-9174 chassis, which transmitted the data to a connected computer. The voltage data was transformed into temperature and velocity measurements, using the Steinhart-Hart equation for the thermistors, and wind-tunnel calibration data for the wind sensor. It is assumed that the foil is thin enough such that the reradiated heat is equal across the two cavities.

## Experimental Method

The Fresnel lamp was placed at a distance of 1850 mm from the glass surface of the apparatus. The foil was measured to receive approximately 100W/m<sup>2</sup> during the arrangement E. The lamp's lens was set to a throw angle of 52° to cover the entire surface of the glass equally, with its power source connected to a transformer set to a constant 240 V. The lamp was switched on to allow the setup to warm up for at least fifteen minutes in order for the system to ensure steady temperature conditions were achieved on the foil. This was confirmed by periodically testing the sensors until consistent temperatures were recorded. Tests were conducted for five minutes, with three repetitions at each position of the air temperature/velocity sensor—220 mm, 550 mm, and 875 mm above the base. A five-minute settling time was allowed after the sensor's location was changed to ensure steady conditions were regained. This process was repeated for each of the tinting configurations illustrated in Figure 2. The grades of tint were achieved by combining multiple layers of tinting film together which compounded the reduction in visible light transmission (VLT). In this experiment, two types of tinting film were used – one which allowed 70% VLT and the other which allowed 15% VLT. The six-level configurations employed a decreasing VLT arrangement beginning with clear glass allowing 100% of light through. This VLT decreased to 70%, 49% (two 70% VLT film - .7<sup>2</sup>), 35% (three 70% VLT film - .7<sup>3</sup>), 24% (four 70% VLT film - .7<sup>4</sup>), 15%, and 2.25% (two 15% VLT film - .15<sup>2</sup>) and a level with no tinting for 100% transmission (Figure 2, configurations A and B). The two-level configurations employed

only the 2.25% arrangement on lower/upper half of the glass and no tint on the upper/lower half of the glass (Figure 2, configurations C and D). A completely untinted glass configuration was also tested (Figure 2, configurations E). These aforementioned tinting configurations were tested in combination with the dual-cavity arrangement while the completely untinted glass configuration was also tested in combination with a single-cavity arrangement (Figure 2, configuration F) in which the rear cavity was blocked at the base, and the air temperature/velocity probe was placed in the front cavity.

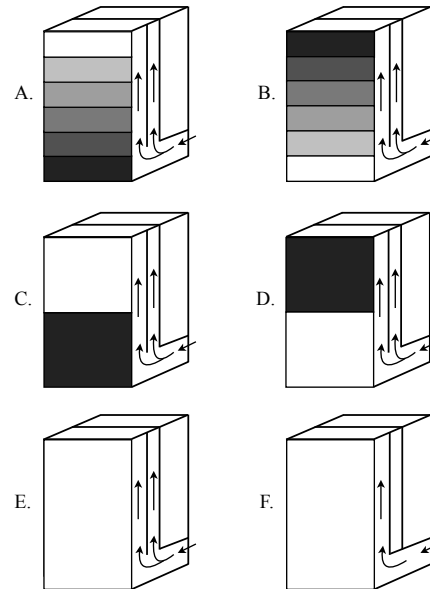


Figure 2. Arrangements of cavities and tinting used in experimentation.

## Results and Discussion

### Effect of single vs. dual cavity

The velocity data (Table 1, and Figure 3) collected for the single-cavity arrangement (configuration F) show that this arrangement had a higher velocity than any of the other dual-cavity arrangements at every measurement. The chief concern of this study, however, is the volumetric flow rate of the system, for which the air velocity is being taken as a proxy measurement. Since the single-cavity arrangement has half the cross-sectional area of the dual-cavity arrangements, with the inlet area remaining constant, the outlet velocity would need to be double that of a dual-cavity system to obtain equal flow rates as per Equation (1)

$$Q = vA \quad (1)$$

Configuration F resulted in an average 29% increase in the velocity compared to E. As the increase was not doubled, this indicates that the single-cavity system does not exhibit a superior flow rate compared to the dual-cavity system. Further testing will be undertaken to confirm the total flow rate of the dual-cavity systems by measuring velocities in both cavities simultaneously.

Considering the temperature data collected from the radiative surface (Table 2, and Figure 4), it was also observed that configuration F recorded higher surface temperatures than configuration E, despite receiving the same solar insolation due to the clear glass.

The retention of heat in the radiative surface indicates that configuration F lost less heat than configuration E to the air stream, and therefore configuration F's single-cavity system is less efficient at heating up the air passing through the cavity—i.e. the single-cavity system obtains less output from the same input

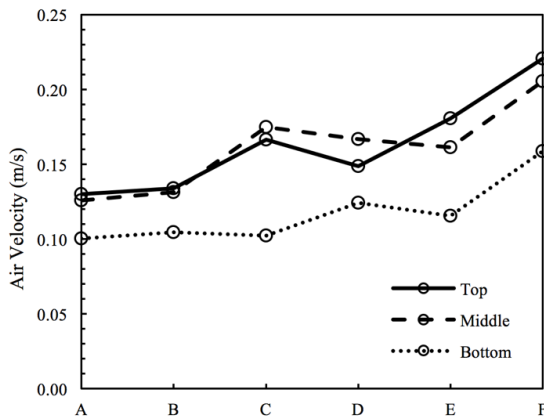


Figure 3. Average air velocities measured at different heights in the cavity for configurations in Figure 2.

Table 1. Average air velocities (m/s) measured at different heights in the cavity for configurations in Figure 2.

	A	B	C	D	E	F
<b>Top</b>	0.1300	0.1339	0.1665	0.1488	0.1806	0.2208
<b>Middle</b>	0.1258	0.1315	0.1748	0.1667	0.1613	0.2055
<b>Base</b>	0.1003	0.1045	0.1024	0.1243	0.1157	0.1589

as the dual-cavity system. This is believed to be due to the halving of the surface area transmitting the heat (i.e. only one side of the foil is heating a moving air stream in the single-cavity system), and the back cavity may be acting as a large air insulator that replenishes the heat lost from the surface. The drop in temperature from the middle to the top of the radiative surface in configuration F may indicate a larger back-flow of cool air from outside the chimney or that the larger velocity caused a rapid loss of heat from the radiative surface.

#### Two-level tinting

Configuration C, tinted at the base and clear at the top, exhibited a lower base velocity and higher top velocity than configuration D, clear at the base and tinted at the top. This can be attributed to the differential insolation experienced by Configuration C's air velocity at the base being hindered by the tint. However, both two-level tinting configurations (C and D) showed the unexpected result of having a higher middle velocity than the clear glass configuration (E).

Configuration C's higher middle velocity may be due to a sudden change in temperature, which would drive the natural convection as described previously. This would in turn produce a pressure-driven stack effect in the form of an increased pressure gradient caused by the greater insolation experienced in the upper part of the shaft—heating the top of the air column more than the base would reduce the density of the air at the top and thereby exaggerate the difference in pressure through the column such that a greater upward movement of air is induced from the region of high pressure (at the base) to the region of low pressure (at the top).

Configuration D's higher middle velocity may be due to a temperature-driven stack effect in which an amplified temperature gradient, caused by the greater insolation of the base of the air column, decreases the density of air at the bottom and increases its buoyancy. The increased buoyancy accelerates the air at the base through the middle of the air column.

In general, it is promising for the two-level tinting concept that the overall envelope of velocities (see Figure 4) is quite similar for configurations C, D and E, i.e. that the two-level configurations are not categorically inferior to the clear-glass configuration.

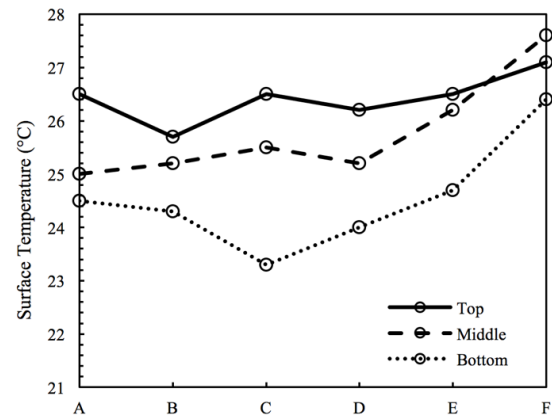


Figure 4. Average surface temperatures measured at different heights along the aluminium foil for configurations in Figure 2.

Table 2. Average surface temperatures (°C) measured at different heights along the radiative surface for configurations in Figure 2.

	A	B	C	D	E	F
<b>Top</b>	26.5	25.7	26.5	26.2	26.5	27.1
<b>Middle</b>	25.0	25.2	25.5	25.2	26.2	27.6
<b>Base</b>	24.5	24.3	23.3	24.0	24.7	26.4

#### Six-level tinting

Configurations A and B were the least successful arrangements, which can probably be attributed to the excessive reduction in total insolation of the radiative surface. By reducing the insolation over so much of the chimney's surface area, it is unlikely that a significant difference in air velocity could have been made by any exaggeration in pressure or temperature gradient that they might also have caused. With the 100% clear level situated mostly below the base of the radiative surface, the surface receives 70% or less VLT along its length. That A & C, and B & D exhibit similar trends (although exaggerated), indicates that even the 2.25% VLT produces a sufficiently large air flow, and that a gradual tint arrangement is not required.

#### Height-dependent velocity and temperature variation

Low temperatures and velocities occurred at the bottom sensor position for all the configurations—even in those configurations of uniform insolation or focussed insolation of the base. The low velocities can be attributed to the cooler incoming air changing direction from horizontal to vertical flow at the base, and the low surface temperature readings to the coolness of the incoming air absorbing more of the heat from the radiative surface, thus reducing the temperature of the foil. The six-level and clear glass configurations showed a consistent acceleration up the air shaft, whereas the two-level configurations exhibited a deceleration of the air stream from the middle to the top; this deceleration may be due, in configuration C, to the lack of buoyancy driving the natural convection flow from below, and in configuration D to the reduction in heating of the air stream at the top due to the decrease in insolation.

A very mild stack effect has also been detected in the apparatus's rest state (i.e. after a significant period without any insolation), in which a temperature variance of ~1-2°C is consistently observed to occur with the bottom surface thermistor the coolest and the top surface thermistor the warmest.

#### Conclusions

The results of the study indicate that the dual-cavity system appears to improve the air flow rate through a solar chimney, but further investigation is required, specifically regarding the simultaneous measurement of velocity in both cavities of the dual-cavity configuration.

A correlation has been found between 2-level tinting and an improvement in air velocity performance above that of the clear-glass configuration in some regions of the air stream, but the specific effect of 2-level tinting is not yet understood. The similarity of the overall envelope of temperatures for configurations C, D and E is promising, and it is hoped that with further refinement of the apparatus and testing of these configurations, the 2-level tinting configurations may be improved to a level of performance that exceeds that of the clear glass—for example, assessing the effect of different heights and levels of transparency of the tinting film.

Along with further refinements of current data collection, the next step for the present research will be the testing of air velocities at a range of distances perpendicular to the radiative surface, to create a comprehensive picture of the flow through the whole cross-section of the cavity and reveal the size and influence of boundary layers along the radiative surface. It is also anticipated that computer simulations that are currently in development will indicate more details of flow patterns throughout the system.

### Acknowledgments

We would like to acknowledge financial support from the School of Civil Engineering at University of Sydney for the experimental setup used in this research.

### References

- [1] Abdelmaksoud, W.A. & Khalil, E.E., Energy savings and thermal comfort optimization in office cubicle environment, *ASHRAE Transactions*, **121**, 2015, 232-240.
- [2] Abedin, M.Z., Tsuji, T. & Hattori, Y., Direct numerical simulation for a time-developing natural-convection boundary layer along a vertical flat plate, *International Journal of Heat and Mass Transfer*, **52** (19-20), 2009, 4525-4534.
- [3] Abedin, M.Z., Tsuji, T. & Lee, J., Effects of freestream on the characteristics of thermally-driven boundary layers along a heated vertical flat plate, *International Journal of Heat and Fluid Flow*, **36**, 2012, 92-100.
- [4] Afonso, C. & Oliveira, A., Solar chimneys: simulation and experiment, *Energy and Buildings*, **32** (1), 2000, 71-79.
- [5] Andersen, K.T., Theoretical considerations on natural ventilation by thermal buoyancy, in *Proceedings of the 1995 ASHRAE Annual Meeting*, 1995, 1103-1117.
- [6] Australian Bureau of Statistics, Environmental Issues: Energy Use and Conservation, in Australian Bureau of Statistics (ed.), Australia 2014.
- [7] Australian Government Department of Environment, *Indoor Air* [Online]. Available: <https://www.environment.gov.au/topics/environment-protection/air-quality/indoor-air> [Accessed 12 May 2016], 2016.
- [8] Bansal, N.K., Mathur, R. & Bhandari, M.S., Solar chimney for enhanced stack ventilation, *Building and Environment*, **28** (3), 1993, 373-377.
- [9] Bassiouny, R. & Koura, N.S.A., An analytical and numerical study of solar chimney use for room natural ventilation, *Energy and Buildings*, **40** (5), 2008, 865-873.
- [10] Bouchair, A., Fitzgerald, D. & Tinker, J., Moving air using stored solar energy, in *Proceedings of the 13th National Passive Solar Conference*, 1988.
- [11] Bouchair, A., Solar chimney for promoting cooling ventilation in southern Algeria, *Building Services Engineering Research and Technology*, **15** (2), 1994, 81-93.
- [12] Burek, S.A.M. & Habeb, A., Air flow and thermal efficiency characteristics in solar chimneys and Trombe Walls, *Energy and Buildings*, **39** (2), 2007, 128-135.
- [13] Chauhan, K., et al., The turbulent/non-turbulent interface and entrainment in a boundary layer, *Journal of Fluid Mechanics*, **742**, 2014, 1-33.
- [14] Chen, Z.D., et al., An experimental investigation of a solar chimney model with uniform wall heat flux, *Building and Environment*, **38** (7), 2003, 893-906.
- [15] Fanger, P.O., *Thermal comfort: analysis and applications in environmental engineering*, New York, McGraw-Hill, 1972.
- [16] Gan, G. & Awbi, H.B., Numerical simulation of the indoor environment, *Building and Environment*, **29** (4), 1994, 449-459.
- [17] Head, M.R., Entrainment in the turbulent boundary layer, *Aeronautical Research Council Reports & Memoranda*, (3152), 1958.
- [18] Ilyas, S., et al., Occupant perceptions of an indoor thermal environment in a naturally ventilated building, *ASHRAE Transactions*, **118**, 2012, 114-121.
- [19] ISO, *ISO 7730: Ergonomics of the thermal environment -- Analytical determination and interpretation of thermal comfort using calculation of the PMV and PPD indices and local thermal comfort criteria*, 2005, International Standards Organisation: Geneva.
- [20] Khanal, R. & Lei, C., A scaling investigation of the laminar convective flow in a solar chimney for natural ventilation, *International Journal of Heat and Fluid Flow*, **45**, 2014, 98-108.
- [21] Nevins, R.G. & McNall, P.E., ASHRAE thermal comfort standards, *Building Research and Practice*, **1** (2), 2008, 100-104.
- [22] Ong, K.S., A mathematical model of a solar chimney, *Renewable Energy*, **28** (7), 2003, 1047-1060.
- [23] Ong, K.S. & Chow, C.C., Performance of a solar chimney, *Solar Energy*, **74** (1), 2003, 1-17.
- [24] Patterson, J.C., et al., Scaling of unsteady natural convection boundary layers with a non-instantaneous initiation, *International Journal of Thermal Sciences*, **48** (10), 2009, 1843-1852.
- [25] Sun, C., et al., A mathematical model to investigate on the thermal performance of a flat plate solar air collector and its experimental verification, *Energy Conversion and Management*, **115**, 2016, 43-51.